

Conformational Analysis of Diterpene Lactone Andrographolide towards Reestablishment of Its Absolute Configuration via Theoretical and Experimental ECD and VCD Methods

Muhamad Faid A Kadir¹, Agustono Wibowo², Fatimah Salim^{3,4}, El Hassane Anouar⁵, Khalijah Awang⁶, Moses Kiprotich Langat⁷, and Rohaya Ahmad^{1,*}

¹Faculty of Applied Sciences, Universiti Teknologi MARA, 40450 Shah Alam, Selangor Darul Ehsan, Malaysia

²Faculty of Applied Sciences, Universiti Teknologi MARA, Pahang Branch, Jengka Campus, 26400 Bandar Tun Abdul Razak Jengka, Pahang Darul Makmur, Malaysia

³Atta-ur-Rahman Institute for Natural Products Discovery (AuRIns), Universiti Teknologi MARA, 42300 Bandar Puncak Alam, Selangor Darul Ehsan, Malaysia

⁴Centre of Foundation Studies, Universiti Teknologi MARA, Selangor Branch, Dengkil Campus 42800 Dengkil, Selangor, Malaysia

⁵Department of Chemistry, College of Sciences and Humanities Studies in Al-Kharj, Prince Sattam bin Abdulaziz University, Al Kharj 11942, Saudi Arabia

⁶Department of Chemistry, Faculty of Science, University of Malaya, 50603 Kuala Lumpur, Malaysia

⁷Jodrell Laboratory, Natural Capital and Plant Health Department, Royal Botanic Gardens, Kew, Richmond, TW9 3DS, UK

* Corresponding author:

tel: +60-355435592

email: rohayaahmad@uitm.edu.my

Received: April 2, 2020

Accepted: August 25, 2020

DOI: 10.22146/ijc.55206

Abstract: Andrographolide, the major constituent from the terrestrial plant *Andrographis paniculata* is a much-studied bioactive ent-labdane diterpene lactone and has become an important medicinal intermediate. As determined by X-ray crystallography, its structure has been applied in molecular docking studies to explain biological activities. Nevertheless, recently, several conflicting reports concerning the stereochemistry at the C-14 and C-10 positions affect the absolute configuration (AC) of the compound. Since a lack of information on the molecular flexibility of the molecule can lead to misleading conclusions on biological activity, a conformational analysis of the molecule in the solution state is necessary. The conformational analysis was performed by the Spartan14 package using the Merck Molecular Force Field (MMFF). The exciton chirality method in electronic circular dichroism spectroscopy (ECM-ECD) and vibrational circular dichroism (VCD) techniques were then jointly employed to re-establish the AC of andrographolide. Theoretical calculations were performed using TD-DFT methods employing the hybrid functionals B3LYP and CAM-B3LYP combined with 6-31G(d,p) basis set. Long-range exciton coupling of 2-naphthoyl chromophores at C-14 and C-19 led to the establishment of the AC to be 3R, 4R, 5S, 9R, 10R, and 14S. Comparison between the theoretical VCD data of **14-S** and **14-R** stereoisomer confirmed a configuration of S at C-14 position instead of R.

Keywords: andrographolide; conformational analysis; exciton coupling; vibrational circular dichroism; absolute configuration

■ INTRODUCTION

Natural products are known as medicinal intermediates, and the determination of their absolute

stereochemistry presents a considerable challenge due to their flexibility in solution state [1-2]. There is an urgency to study the conformational analysis of

bioactive chiral molecules in the solution state in which the bio-activity is observed since it will affect their absolute configuration. The correct stereochemistry is crucial for the understanding of the bioactivity of chiral compounds via molecular docking studies.

ECD and VCD are highly sensitive techniques in investigating the molecular conformation, configuration, solvation, and aggregation of chiral molecules [3]. Both ECD and VCD spectra allow the assignment of absolute stereochemistry determination feasible and conformational analysis in a solution for a compound alongside NMR (1D & 2D) experiments leading to relative stereostructure determination [4]. In addition, ECD provides a powerful tool for the AC assignment to chiral molecules in solution form as the chemical properties of chiral compounds are more clearly interpreted without the crystallization or the use of chiral auxiliaries for which single crystal X-ray methods are not applicable. The limitation of ECD is the requirement of a strong UV-Vis chromophore. However, this can be overcome by attaching chromophores to the molecule, as applied in the exciton chirality method (ECM-ECD method).

While the VCD technique offers the same benefits as ECD, it is not as sensitive as ECD, but it is applicable to most organic compounds capable of IR absorption. Furthermore, VCD also provides more spectral peaks with high signal resolution and good conformational sensitivity for chiral molecules compared to ECD, which helps reduce the efforts to determine the AC [5]. For both techniques, the interpretation of resulting spectra is nevertheless compromised by the number of overlapping transitions. Therefore, ECD and VCD spectra are most often compared to theoretical spectra calculated by applying first-principles theory *ab initio* methods by quantum mechanics (QM) [6-7].

Diterpenes are bicyclic compounds widely recognized as bioactive natural products. For these chromophore-lacking compounds, the application of ECM-ECD technique for its AC determination via long-range coupling of attached chromophores seemed feasible. Due to its important role as a medicinal intermediate and the absence of reports for its conformational analysis in the solution form,

andrographolide was chosen to be studied. The AC of the molecule was first determined by X-ray crystallography more than three decades ago [8-9]. While the early study reported by Fujita et al. [9] suggested an *R* configuration at the C-14 position, a 3D structure indicates the opposing *S* configuration. Similarly, a recent report [10] assigned the stereochemistry at the C-10 position as *S* via X-ray crystallography, which is inconsistent with a regular *ent*-labdane structure.

In this study, 2-benzoyl and 2-naphthoyl chromophores were employed with moderate electric dipole moments (2.24D & 5.07D) for the derivatization of the lactone to yield four derivatives via the ECM-ECD technique. The conformational analysis of each derivative was then carried out, and the experimental and theoretical ECD data were compared. As a complementary method, the experimental and theoretical VCD spectra of andrographolide **1** were also obtained to deduce the AC of the labdane diterpene lactone. In addition, the theoretical VCD data for its C-14 stereoisomer **Iis-14** was also calculated to confirm the stereochemistry at C-14.

■ EXPERIMENTAL SECTION

Material

All the chemicals used in this work were of analytical grade. The plant material (aerial parts of *Andrographis paniculata*) was obtained from Sungai Petani, Kedah, Malaysia. This specimen was supplied to the Herbarium Unit, Department of Botany, University of Malaya, with herbarium series number KL4930. The plant was dried for four days and ground into a fine powder.

Instrumentation

ECD data were collected on a JASCO J-815 CD spectropolarimeter with λ_{\max} ($\Delta\epsilon$) in the range of 190–400 nm. VCD measurements were done on a JASCO FVS-6000 (JASCO Inc, Mary's Court Easton, MD, USA). NMR spectra were recorded on a JEOL ECZS400 400 MHz spectrometer operating at 400 (^1H) and 100 (^{13}C) MHz equipped with shims gradient selective ^2H and ^1H

series and autosampler. 2D NMR experiments were performed using standard JEOL programs. All measurements were carried out at 291.15 K. Chemical shifts were reported as δ values (ppm) with the residual solvent signal and tetramethylsilane (TMS) as internal reference. *J*-coupling in Hz, and standard pulse sequences from the Delta NMR processing and control (v5.0.4.4, windows) software package were used (JEOL Inc., Peabody, MA, USA).

Procedures

Isolation of andrographolide

Two kilograms (2 kg) of dried *A. paniculata* powder was soaked in methanol (100%) for 3 days. The liquid extract was then filtered, and the solvent was removed at reduced pressure. This first procedure was repeated five times until a clear solution was obtained. Next, an aqueous solution of the dried methanol extract was subjected to liquid-liquid partitioning with hexane, dichloromethane (DCM), and ethyl acetate (EA) to yield the hexane, DCM, and EA extracts, respectively, upon evaporation of the solvent. The EA fraction (15 g) was then subjected to column chromatography with solvent system CHCl_3 :Acetone:MeOH, 7:3:1, which produced the best separation on TLC. Fifty fractions were collected, and each fraction was left to dry. Next, the combined fraction of 10–20 was subjected to centrifugal preparative TLC (CHCl_3 :MeOH, 9.5:0.5) followed by recrystallization (using EA as solvent) to yield andrographolide **1** (396 mg). The relative structure of the known andrographolide was confirmed by 1D and 2D NMR spectroscopy.

Chromophoric derivatization of andrographolide

Andrographolide (15 mg, 42.8 μmol) dissolved in 5 mL of anhydrous acetonitrile together with triethylamine (29.82, 5 eq) were added in a 25 mL round bottom flask. After 5 min of stirring, benzoyl chloride (29.83 μL , 6 eq) was added. The mixture was stirred at room temperature for 24 h in a nitrogen environment, and the reaction was monitored by TLC (silica gel, UV detection, and CrSO_4 as spraying reagent). Products **2** and **3** were purified using radial chromatography with solvent system CHCl_3 :MeOH, 9.5:0.5. Structure elucidation of the products was carried out using 1D and 2D NMR spectroscopy. The

same method was applied to the chromophore 2-naphthoyl chloride to yield derivatives **4** and **5**.

Computational analysis

The initial conformational analysis was performed by the Spartan '14 package using the MMFF molecular mechanics force field of *Monte Carlo* protocol. After collecting and selecting the conformational distribution calculated, the conformers within 2 kcal/mol range from the global minimum window were chosen and subjected to energy minimization using DFT calculations as implemented in the Gaussian 09W package.

Theoretical calculations of ECD and VCD spectra were performed by Gaussian 09W at the TDDFT level of theory using either the B3LYP (gaseous phase) or CAM-B3LYP (solvent phase) functionals, and suitable selection of basis set; 6-31+(d,p). The use of the long-range corrected CAM-B3LYP (solvent phase) functional was predicted to provide better ECD spectra simulation results than the more common B3LYP functional. For each optimized conformer, the excitation energy (in nm) and rotatory strength *R* (unit: 10–40 cgs) in the dipole velocity (*R_{vel}*) and dipole length (*R_{len}*) forms were calculated in acetonitrile (CH_3CN) by TDDFT/B3LYP/6-31G**, using the SCRF method, with the CPCM model. The theoretical CD spectra were obtained as weighted averages of Boltzmann populations. The final results of the calculated spectra were compared with experimental CD spectra to establish the AC of the selected compound [1,5].

RESULTS AND DISCUSSION

ECM-ECD Analysis of 1-5

Andrographolide **1** (Fig. 1) is a labdane-type diterpene and is widely recognized as a bioactive natural product [11-12]. The experimental ECD spectrum of **1** did not give much valuable information for AC determination. Furthermore, the spectrum results from the $\pi \rightarrow \pi^*$ electronic transitions of 'ene' lactone moiety at the furanone ring, which does not significantly represent the absolute configuration of the global molecule structure. The sensitivity of **1** towards ECD analysis is expected to increase by replacement of hydrogen atoms of hydroxyl groups at C-14 and C-19

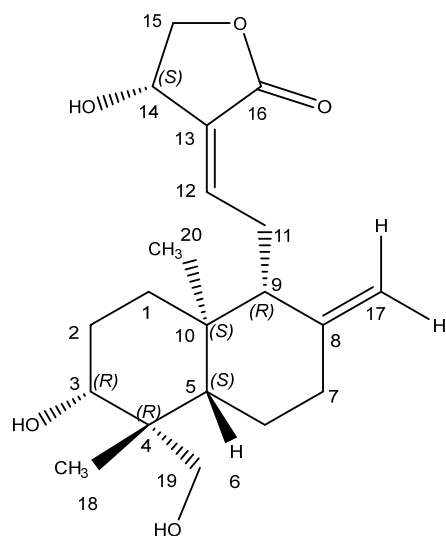
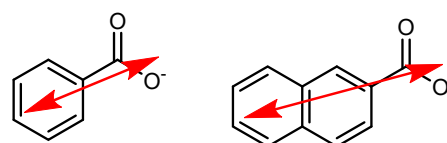


Fig 1. Chemical structure of andrographolide (**1**) with carbon numbering. The configuration was determined using single-crystal X-ray crystallographic technique from previous studies

carbon atoms (bond distance $\sim 8 \text{ \AA}$) by the selected chromophores (Fig. 2) as the steric hindrance for both deprotonated hydroxyl groups is relatively low. Thus, they can exist as stable nucleophiles. For anticipating this, 4 andrographolide derivatives (**2–5**) were successfully synthesized (Fig. 3) according to standard methodologies yielding products with a yield of 50–70%. The structures of **2–5** were confirmed by 1D and 2D NMR data (See Supplementary Materials).

Upon confirmation of their structures, the derivatives were subjected to ECD analysis. All four derivatives (**2–5**) showed a good CE split (bisignate curve)

at maximum absorbance between 210–240 nm with a higher intensity as compared to **1** at the same concentration of 0.03 mM (Fig. 4). Having additional chromophores has thoroughly increased the sensitivity of selected compounds at the minimum concentration (UV absorption intensity = 0.6–1.4). In contrast, the strength of electric dipole moments, interchromophoric distance, and chiral dihedral angle are the key factors that affect the total exciton coupling between the two chromophores, although their position in space is relatively near/far to each other [13–14]. Nevertheless, all the CE observed (Fig. 4) for all four derivatives showed negative first maxima at λ_{max} 236 nm ($\Delta\epsilon$ -20.9), λ_{max} 235 nm ($\Delta\epsilon$ -47.3), λ_{max} 243 nm ($\Delta\epsilon$ -30.3) and λ_{max} 240 nm ($\Delta\epsilon$ -70.7), respectively. This data indicates that the dihedral twist between the chromophores is arranged in space in a counter-clockwise manner. Interestingly, it is observed that the ECD signals for **2**, **3**, and **4** did not show a very distinguishable bisignate CE



Name	Benzoyl ester	Naphthoyl ester
λ_{max}	230 nm	239 nm
Dipole moment	2.24 D	5.07 D

Fig 2. Selected chromophores chosen for exciton-coupled circular dichroism method. Red arrows show the electric transition dipole (dipole moment was calculated by semi-empirical method using Spartan '14)

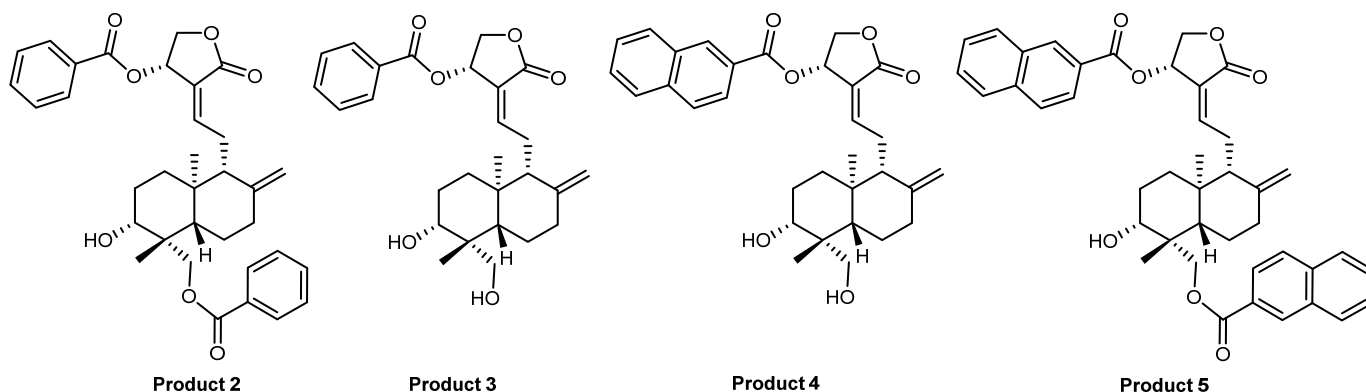


Fig 3. Chemical structures of andrographolide derivatives (**2–5**). Derivatives **2** and **3** and derivatives **4** and **5** were obtained from single reaction of different chromophores used for derivatization

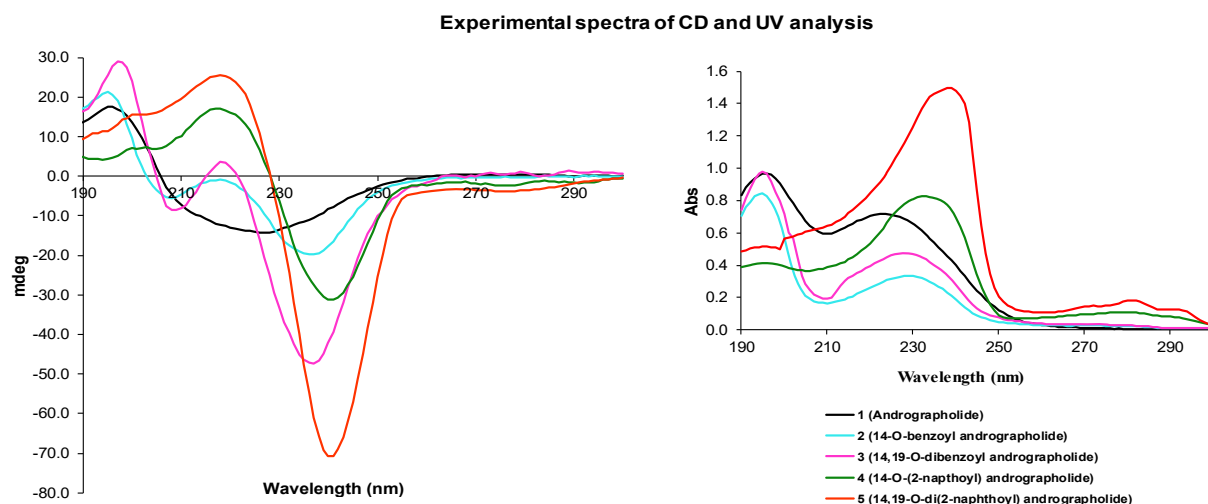


Fig 4. Experimental CD (left) and UV (right) spectra of compounds 1–5. CD analysis were done in acetonitrile as solvent and the concentration was constant at 0.03 ppm. The wavelength was collected between 190–400 nm and only significant absorption up to 300 nm was considered

to allow the elucidation of the AC of the whole molecular structure while the spectrum observed for **5** is conclusively intense and distinguishable.

The exciton couplet from the interaction between two 2-naphthoyl ester chromophores in the skeleton of **5** showed an intense and good distinct negative CE (243 nm $\Delta\epsilon$ -70.7 and 218 nm $\Delta\epsilon$ +25.5) around the UV maximum (λ_{max} of 240 nm), suggesting the *S*-absolute and *R*-absolute configuration of chiral centers C-14 and C-4, respectively (Fig. 5). These assignments are in accordance with previous studies in terms of 3D structures [8-9]. However, Fujita et al. [8] described the stereochemistry at C-14 as *R*. Furthermore, the results suggest how 2-naphthoyl ester structures introduced to **1** restrict the space rotation flexibility and rationalize the absolute configuration within a distance of 8 Å [13,15].

The experimental data agreed well with predicted ECD spectra using time-dependent density functional theory (TD-DFT) calculation. A conformational analysis study was first carried out in order to reduce the uncertainty and determine the conformer distribution in the solution state at room temperature. Geometry optimization was carried out to reduce the calculation period for the conformer distribution population. Thereafter, the calculation was calculated in the protocol

of *Monte Carlo* to reduce the computational effort in the conformational analysis [5,16-18].

Structure **5** was defined as a tweezer-like structure based on the negative chirality data obtained and 3D structure drawn from the conformational analysis. Prediction on the minimal energy optimization of **5** showed that the Boltzmann distribution for conformers was predominated by the tweezer-like structure in a negative chirality manner within the minimum energy

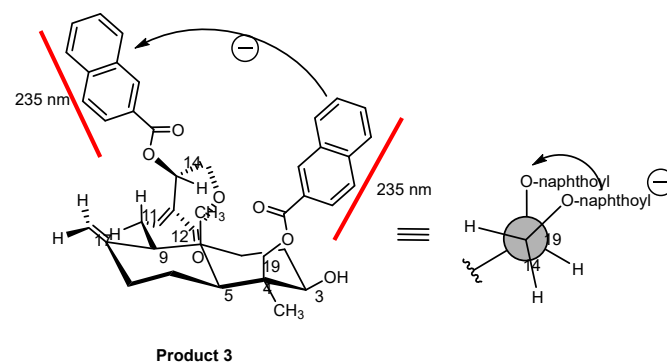


Fig 5. Negative chirality of **5** resulting from exciton coupling of two chromophores with interchromophoric distance 8 Å. Anticlockwise coupling from the front view of chromophoric couple indicates the negative chirality. The structure and interchromophoric distance were determined using ChemDraw software

of 2 kcal/mol. The postulated structure of **5** suggests that the dihedral angle of the coupling electric-dipole transition moment contributed to the perturbation of the negative ECD spectrum. In addition, specific properties of the steric arrangement for both 2-naphthoyl ester rings in **5** that are not parallel to each other (energy minimization) likely reduce the flexible rotation of the whole molecule and ease the calculation of theoretical ECD spectra [19-20]. There was no change in the number of conformers for Structures **4** and **5**.

Table 1 shows the conformer distribution of **1** and its derivatives. As shown in this table, the monosubstituted andrographolide derivatives **2** and **4** possess six and four conformers, respectively. Meanwhile, the disubstituted andrographolide derivatives **3** and **5** have five and four conformers, respectively. The different number of stable conformers within the energy of 2 kcal/mol was governed by the geometric flexibility of the calculated molecules. For derivative **5**, its large structure with a higher dipole moment of chromophore introduced has significantly hindered the conformer flexibility as the couple and interact spatially through space. Besides that, the first conformer of **5** (CF1), possessing the least energy, shows high Boltzmann distribution (> 0.5) which indicates geometry dominance in nature [17,21-22].

The ECD spectra were predicted at the B3LYP/6-311+G(d,p) level of theory in the gas phase initially followed by calculations within the PCM solvation model of acetonitrile for each compound. Based on the experimental ECD spectra of **1-5**, which were used as

diagnostic chirality markers, the simulated spectra were expected to produce negative CE. Additionally, **5** is expected to exhibit a good bisignate CE in the context of the exciton coupling method [1-2]. Upon comparison, the overall pattern of simulated ECD spectra was in excellent agreement with the experimental spectra of **1-5** (Fig. 6). The predicted spectra for **4** and **5** showed a bisignate CE similar to that observed in the experimental data. Furthermore, CF1 of **5** exhibited the highest percentage agreement, and the Boltzmann distribution resulted in more than 50% population where it is considered more reliable for AC determination in nature.

Experimental VA and VCD Analysis of **1**

The vibrational absorbance (VA) and vibrational circular dichroism (VCD) spectra of **1** were recorded in solution (DMSO-*d*₆) to replicate the properties of the tested compound in a non-rigid chemical environment at a controlled temperature (25.0 °C) with a band resolution of 4.0 cm⁻¹. The sample concentration was tested initially at 1.0 M at 50 µL to identify the weak signal throughout the full range of the spectrum (800–2000 cm⁻¹). Then, the concentration was gradually reduced down to 0.1 M to measure the specific region with strong vibrational absorbance in order to obtain reliable data of strong VCD signal.

The initial VA analysis measured using the KBr plate method showed a good absorption in the mid-IR region (800–2000 cm⁻¹). From the VA spectra of **1**, five

Table 1. The energy conformations of andrographolide derivatives **2-5** with Boltzmann distribution to indicate the conformer stability after geometry optimization at minimum energy configuration where Rel. E represents the relative energy

Conformer No.	2			3			4			5		
	Energy (kcal/mol)		Boltz. Dist									
	E	Rel. E		E	Rel. E		E	Rel. E		E	Rel. E	
CF1	107.20	0.00	0.429	137.37	0.00	0.387	157.92	0.00	0.537	157.92	0.00	0.537
CF2	107.33	0.13	0.343	137.45	0.09	0.335	158.26	0.34	0.301	158.26	0.34	0.301
CF3	108.09	0.89	0.096	138.01	0.64	0.132	159.15	1.23	0.067	159.15	1.23	0.067
CF4	108.43	1.24	0.053	138.07	0.47	0.119	159.44	1.53	0.041	159.44	1.53	0.041
CF5	108.45	1.25	0.052	139.20	1.83	0.018	-	-	-	-	-	-
CF6	109.10	1.91	0.017	-	-	-	-	-	-	-	-	-

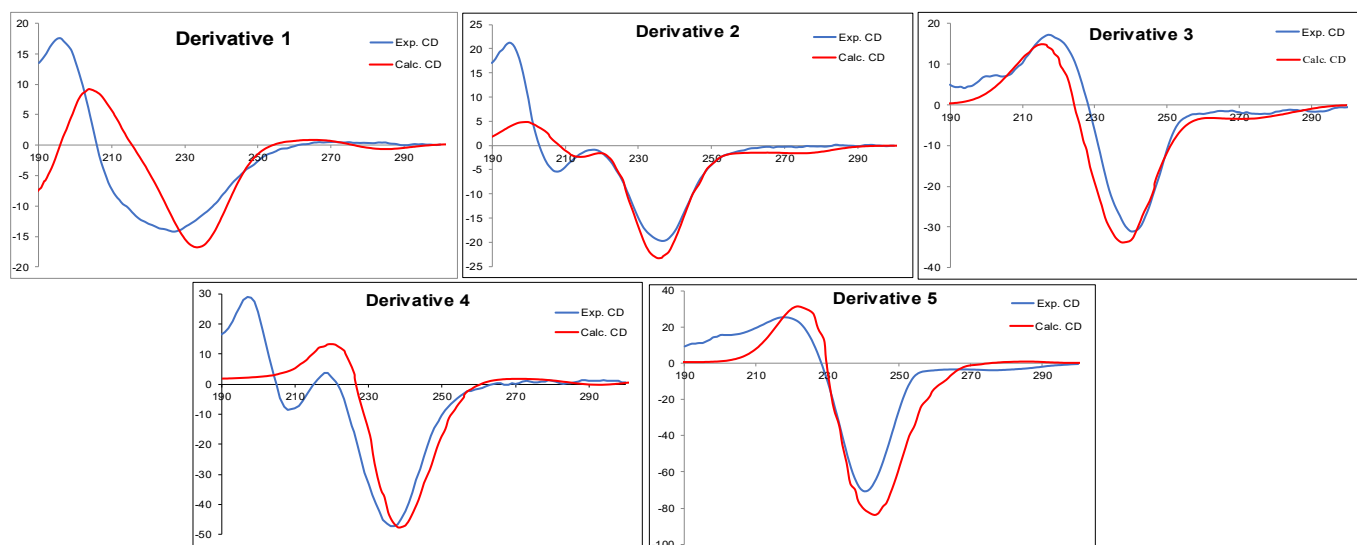


Fig 6. Experimental (blue) and Boltzmann weighted calculated (black) ECD spectra for **5**. Experimental in acetonitrile, simulated calculated with TDDFT/B3LYP//6-311+G(d,p)

strong and medium peaks were selected as a reference before the analysis was carried out in the solution state. A strong peak was observed at 1727.80 cm^{-1} , which represent stretching energy from the conjugation of ester carbonyl functional group at C-16. Other characteristic peaks are seen as sharp peaks at 3398.98 and 2928.06 cm^{-1} represent -OH and C-H stretching. In addition, the pattern of peaks in the near IR region stipulates that **1** is involved in a number of intramolecular hydrogen bonding specifically for hydroxyl group for C-3 and C-19 that are naturally positioned near each other in space. Although there are a few strong and sharp absorption peaks that can be observed from $2800\text{--}3400\text{ cm}^{-1}$, it is relatively uncommon to analyze VCD absorption at this region due to unstable and broad vibrational absorption. This region is also routinely neglected or only considered for certain and complicated cases. This is mainly caused

by the fact that this region does not fully represent the vibration energy on total chemical structure and sensitive towards the hydrogen bonding vibration specifically for molecules that contain hydroxyl groups like **1**. Other important considerations are the type of bonding directly attached to chiral centers, i.e., C-O, C-C, C-H bending energy. Table 2 gives comprehensive data of characteristic peaks identified by their type of bonding vibration energy and their contribution to chirality, indicating direct attachment or involvement of functional structure in chiral rotation and configuration.

VCD analysis of **1** was recorded at 48000 scan number, which is equivalent to 8 h. As reported by García-Sánchez et al., 2014 [23], other labdane diterpenes may take 6 to 11 h of VCD analysis period depending on the flexibility of the compound tested. This phenomenon due to the fact that the vibrational transition of chemical

Table 2. VA Peak characterization of **1** using KBr plate method

Band number	Experimental frequency	Vibrational origin	Contribution to chirality
1	3398.98	O-H stretching	Positive
2	2928.06	C-H stretching, sp^3	Positive
3	1727.80	C=O stretching of carbonyl ester	Positive
4	1674.67	C=C stretching, sp^2	Negative
5	1221.01	=C-O stretching	Positive
6	1032.98	C-O alkoxy stretching	Positive
7	980.85	CH out of plane bending for trans alkene	Negative

bonding is a weak quantized energy produced by electron wavefunction [24]. Rationally, as the number of scans increases, more data can be collected, repeated to improve the signal-to-noise (S/N) ratio and produce VCD at a higher intensity. However, due to solvent effects, the vibrational absorbance at region $800\text{--}1000\text{ cm}^{-1}$ could not be obtained clearly, and this minimal complication usually has no negative upshot of total VCD spectra.

Furthermore, the natural existence of C=O group in **1** can significantly improve the VCD assignment since the signal produced is alienated from the fingerprint region. A good band-to-band comparison of calculated and experimental VCD spectra is very important for configuration assignment since calculated frequencies are derived from a harmonic force field. In contrast, calculated IR and VCD frequencies are derived from a non-harmonic force field from the bending or stretching. Thus, the uncertainty of VCD experimental analysis can be justified by the calculated spectra and thereby establishing absolute configuration [23].

Theoretical VCD Calculation of **1** and Its C-14 Stereoisomer

The calculated VA and VCD spectra were done at a similar functional theory level as the previous ECD calculation, CAM-B3LYP/6-311+G(d,p). The vibrational response resulted in five clear VA bands and corresponding VCD peak from which a peak for the carbonyl band gave rise to an isolated VCD peak. However, the peaks in the fingerprint region were more congested, and the VCD response for both experimental and simulated could not be seen clearly. Some broad and yet weak peak fairly envelope in the region $\sim 1300\text{ cm}^{-1}$. Their appearance may be attributed to the presence of closely spaced vibration bands between the conformers. The total populated calculation led to the conclusion that

the latter rationale is more applicable to the study of other stereoisomers [25], thus reconfirming the reliability of calculated VCD spectra of **1**.

Table 3 shows the conformer distribution of **1** and its theoretical stereoisomers. The most prominent peaks were observed in the carbonyl region, giving rise to a VCD response. The theoretical vibrational energy was calculated for a stereoisomer of **1** with an *R* configuration for C-14. The analysis of **1** with the theoretical isomers was prominent as a tool for observing the vibrational energy region involved in changing the pattern of calculated VCD data obtained. However, observation in the region $2800\text{--}3500\text{ cm}^{-1}$ was also taken into account to pinpoint whether its contribution in VCD analysis was relevant for the AC assignment. From the structure modification, only calculated VCD data were affected, while no apparent changes can be observed from calculated VA data.

The method of primary VCD calculation was used for this section to ensure the results obtained did not contradict with andrographolide VCD calculation. Furthermore, calculation with a similar method was more reliable for the different signals of simulated VCD comparison. After geometry optimization and conformational search, the two proposed stereoisomers were subjected to VCD analysis. Comparing the two stereoisomers helps improve the data confidence level and deduce the correct stereochemistry at C-14.

Fig. 7 shows the spectral agreement of VA and corresponding VCD of **1** at the region $1600\text{--}1700\text{ cm}^{-1}$ and the difference between the theoretical calculation for **1** and **Iis-14**. The key peaks from the spectra are shown in Table 3S (Supplementary Materials). The spectra in black represent the experimental, while the spectra in blue represent the calculated spectra of both

Table 3. Conformer distribution of **1** and its theoretical stereoisomers

Stereoisomers	1	Iis-14	Stereoisomers	1	Iis-14
CF1	0.281	0.750	CF6	0.047	-
CF2	0.200	0.241	CF7	0.043	-
CF3	0.139	0.003	CF8	0.034	-
CF4	0.054	0.002	CF9	0.032	-
CF5	0.047	0.002	CF10	0.017	-

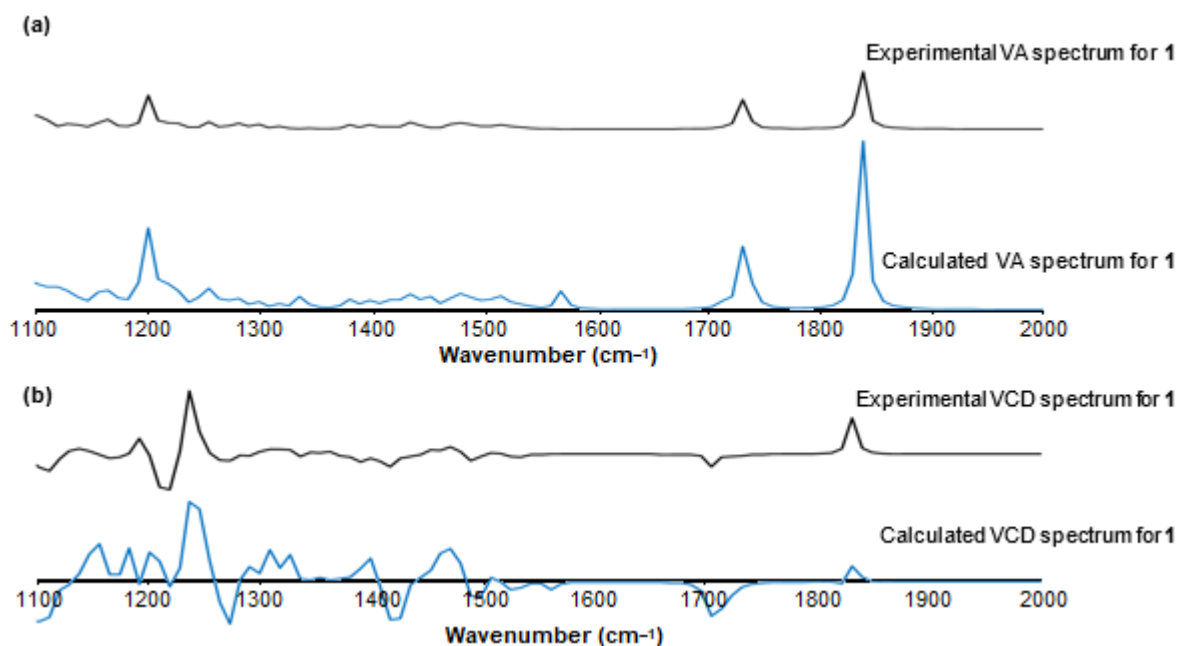


Fig 7. Experimental (black) and calculated (blue) VA (a) and VCD (b) spectra of andrographolide (**1**)

VA and calculated VCD spectra of **1** and **1is-14** weighted from the ten and six conformers from the global window, respectively. Clear correlations can be seen at the region 1700–1900 cm^{-1} . In the fingerprint region, only one peak was prominent. Experimental analysis of VA and VCD was done for 1 min at 32 and 8 h at 48000 scan numbers, respectively, using BaF₂ glass cuvette with a pathlength of 50 μm . The absorption intensity of the experimental spectra was slightly weaker than the calculated data. These results were consistent with literature that focused on the VCD of labdane-type diterpene compound for AC determination [23,25]. The chemical environment, such as the solvent employed, is one reason why infrared energy was not absorbed for the vibrational transition within the molecule. Nonetheless, VA and VCD spectra have a similar pattern from 1100–2000 cm^{-1} , which clearly justifies the liability of the experimental analysis.

The two stereoisomers produced a variable pattern of VCD spectra. Two pivotal peaks at $\sim 1700 \text{ cm}^{-1}$ were used as the primary reference for the VCD response of all stereoisomers. VA signals above 2800 cm^{-1} did not seem to have a significant contribution towards VCD analysis. Likewise, the unique pattern of coupled VCD response at $\sim 1700 \text{ cm}^{-1}$ provided important information for the differentiation between andrographolide and its C-14

isomer **1is-14**. However, the intensity of VCD response for **1is-14** was comparatively higher than **1**.

Some observations can be made from the region 1600–1900 cm^{-1} (C=O stretching), where the VCD response was seen as two distinct peaks. Each stereoisomer has different peak order (+/-, +/+, -/+, -/-) and is easily compared as they were excluded from the fingerprint region. Nevertheless, the order of VCD peak in the carbonyl region for both **1** and **1is-14** is identical (-/+). Thus, the signal which lay within the fingerprint region was used to differentiate between the two stereoisomers, although the VCD response for **1** was slightly weaker than **1is-14**. We have shown that comparing theoretical data between stereoisomers is critical to avoid a mismatched assignment in determining absolute configuration.

CONCLUSION

The conformational analysis of andrographolide derivatives and re-establish its AC were carried out in the solution state via the joint ECM-ECD and VCD techniques. The attachment of 2-naphthoyl group at C-14 and C-19 in derivative **5** was found to reduce its molecular flexibility and the number of conformers resulting in four conformers with relative energy less

than 2 kcal. Conformer 1 (CF1) was found to possess the least energy and had the highest Boltzmann distribution (> 0.5), which indicates geometry dominance in nature. Due to its higher electric transition dipole moment, exciton coupling observed between the 2-naphthoyl moieties produced a more significant bisignate CE than between the benzoyl groups. Long-range exciton coupling of 2-naphthoyl chromophores at C-14 and C-19 in derivative **5**, using the ECM-ECD technique, led to the establishment of the AC to be 3*R*, 4*R*, 5*S*, 9*R*, 10*R*, and 14*S*. In the VCD method, a relatively good match was found between the experimental spectra and the theoretical spectra of **1** performed at the TDDFT level of theory using the long range corrected CAM-B3LYP (solvent phase) functionals and basis set; 6-311+G(d,p). Comparison between the theoretical VCD spectra for **1** and **Iis-14** further minimizes the possibility of a 14*R* configuration for andrographolide.

■ ACKNOWLEDGMENTS

This work was fully supported by the Ministry of Higher Education, Malaysia (MOHE) under FRGS and BESTARI Grant, Ref: 600-RMI/FRGS5/3(49/2013) and 600-IRMI/DANA5/3/BESTARI(0028/2016), respectively.

AUTHOR CONTRIBUTIONS

MFAK conducted the experiment and drafted the manuscript, AW carried out chromophoric derivitization and assisted with NMR interpretation, FS assisted with the CD experiments, E-HA conducted conformational analysis and the DFT calculations, KA assisted in the project design, ML assisted with the interpretation of ECD spectra, RA designed the project and revised the manuscript. All authors agreed to the final version of this manuscript.

■ REFERENCES

- [1] Anouar, E.H., and Weber J.-F.F., 2013, Time-dependent density functional theory study of UV/vis spectra of natural styrylpyrones, *Spectrochim. Acta, Part A*, 115, 675–682.
- [2] Pescitelli, G., Di Bari, L., and Berova, N., 2011, Conformational aspects in the studies of organic compounds by electronic circular dichroism, *Chem. Soc. Rev.*, 40 (9), 4603–4625.
- [3] Bultinck, P., Cherblanc, F.L., Fuchter, M.J., Herrebout, W.A., Lo, Y.P., Rzepa, H.S., Siligardi, G., and Weimar, M., 2015, Chiroptical studies on brevianamide B: Vibrational and electronic circular dichroism confronted, *J. Org. Chem.*, 80 (7), 3359–3367.
- [4] Mishra, S.K., and Suryaprakash, N., 2017, Some new protocols for the assignment of absolute configuration by NMR spectroscopy using chiral solvating agents and CDAs, *Tetrahedron: Asymmetry*, 28 (10), 1220–1232.
- [5] Petrovic G.A., Navarro-Vazquez, A., and Alonso-Gomez J.L., 2010, From relative to absolute configuration of complex natural products: Interplay between NMR, ECD, VCD, and ORD assisted by ab initio calculations, *Curr. Org. Chem.*, 14 (15), 1612–1628.
- [6] Batista, J.M., and da Silva Bolzani, V., 2014, Chapter 13. Determination of the absolute configuration of natural product molecules using vibrational circular dichroism, *Stud. Nat. Prod. Chem.*, 41, 383–417.
- [7] Salim, F., Yunus, Y.M., Anouar, E.H., Awang, K., Langat, M., Cordell, G.A., and Ahmad, R., 2019, Absolute configuration of alkaloids from *Uncaria longiflora* through experimental and theoretical approaches, *J. Nat. Prod.*, 82 (11), 2933–2940.
- [8] Smith, A.B., Toder, B.H., Carroll, P.J., and Donohue, J., 1982, Andrographolide: An X-ray crystallographic analysis, *J. Crystallogr. Spectrosc. Res.*, 12 (4), 309–319.
- [9] Fujita, T., Fujitani, R., Takeda, Y., Takaishi, Y., Yamada, T., Kido, M., Miura, I., 1984, On the diterpenoids of *Andrographis paniculata*: X-ray crystallographic analysis of andrographolide and structure determination of new minor diterpenoids, *Chem. Pharm. Bull.*, 32 (6), 2117–2125.
- [10] Chantrapromma, S., Boonnak, N., Pitakpornprecha, T., Yordthong, T., Kumar, C.S.C., and Fun, H.K., 2018, Absolute configuration of andrographolide and its proliferation of

- osteoblast cell lines, *Crystallogr. Rep.*, 63 (3), 416–421.
- [11] Jayakumar, T., Hsieh, C.Y., Lee, J.J., and Sheu, J.R., 2013, Experimental and clinical pharmacology of *Andrographis paniculata* and its major bioactive phytoconstituent andrographolide, *Evid. Based Complement. Altern. Med.*, 2013, 846740.
- [12] Hossain, M.S., Urbi, Z., Sule, A., and Rahman, K.M.H., 2014, *Andrographis paniculata* (Burm. f.) Wall. ex Nees: A review of ethnobotany, phytochemistry, and pharmacology, *Sci. World J.*, 2014, 1–28.
- [13] Berova, N., Ellestad, G.A., and Harada, N., 2010, “Characterization by circular dichroism spectroscopy” in *Comprehensive Natural Products II: Chemistry and Biology*, Eds. Mander, L., and Liu, H.W., Elsevier Science, United Kingdom, 91–146.
- [14] Berova, N., Polavarapu, P.L., Nakanishi, K., and Woody, R.W., 2012, *Comprehensive Chiroptical Spectroscopy: Applications in Stereochemical Analysis of Synthetic Compounds, Natural Products, and Biomolecules*, John Wiley & Sons, Inc., Hoboken, New Jersey, United States.
- [15] Li, X., Burrell, C.E., Staples, R.J., and Borhan, B., 2012, Absolute configuration for 1, *n*-Glycols: A nonempirical approach to long-range stereochemical determination, *J. Am. Chem. Soc.*, 134 (22), 9026–9029.
- [16] Tanaka, H., Inoue, Y., Nakano, T., and Mori, T., 2017, Absolute configuration determination through the unique intramolecular excitonic coupling in the circular dichroisms of *o,p'*-DDT and *o,p'*-DDD. A combined experimental and theoretical study, *Photochem. Photobiol. Sci.*, 16 (4), 606–610.
- [17] Autschbach, J., 2009, Computing chiroptical properties with first-principles theoretical methods: Background and illustrative examples, *Chirality*, 21 (1E), E116–E152.
- [18] Taniguchi, T., 2017, Analysis of molecular configuration and conformation by (electronic and) vibrational circular dichroism: Theoretical calculation and exciton chirality method, *Bull. Chem. Soc. Jpn.*, 90 (9), 1005–1016.
- [19] Pescitelli, G., Di Bari, L., and Barova, N., 2014, Application of electronic circular dichroism in the study of supramolecular systems, *Chem. Soc. Rev.*, 43 (15), 5211–5233.
- [20] Nicu, V.P., and Jan Baerends, E., 2011, On the origin dependence of the angle made by the electric and magnetic vibrational transition dipole moment vectors, *Phys. Chem. Chem. Phys.*, 13 (36), 16126.
- [21] Person, R.V., Monde, K., Humpf, H., Berova, N., and Nakanishi, K., 1995, A new approach in exciton-coupled circular dichroism (ECCD)-Insertion of an auxiliary stereogenic center, *Chirality*, 7 (3), 128–135.
- [22] Berova, N., Nakanishi, K., and Woody, R.W., 2000, *Circular Dichroism. Principles and Applications*, 2nd Ed., John Wiley & Sons, Inc., New York, US.
- [23] García-Sánchez, E., Ramírez-López, C.B., Talavera-Alemán, A., León-Hernández, A., Martínez-Muñoz, R.E., Martínez-Pacheco, M.M., Gómez-Hurtado, M.A., Cerda-García-Rojas, C.M., Joseph-Nathan, P., and del Río, R.E., 2014, Absolute configuration of (13*R*)- and (13*S*)-labdane diterpenes coexisting in *Ageratina jocosotepecana*, *J. Nat. Prod.*, 77 (4), 1005–1012.
- [24] Hoffmann, S.V., Fano, M., and Van de Weert, M., 2016, “Circular dichroism spectroscopy for structural characterization of proteins” in *Analytical Techniques in the Pharmaceutical Sciences. Advances in Delivery Science and Technology*, Eds. Müllertz, A., Perrie, Y., and Rades, T., Springer, New York, NY, 223–251.
- [25] Joseph-Nathan, P., Gordillo-Román, B., 2015, Vibrational circular dichroism absolute configuration determination of natural products, *Prog. Chem. Org. Nat. Prod.*, 100, 311–452.